Calculation of bulk properties of liquids and supercritical fluids from pure theory

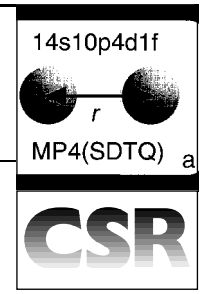

Hanspeter Huber, Anthony J. Dyson and Barbara Kirchner

Institut für Physikalische Chemie der Universität Basel, Klingelbergstr. 80, CH-4056 Basel, Switzerland

Received (in Cambridge) 8th May 1998

Wouldn't it be nice if we could determine the molar heat capacity or the viscosity of a liquid purely from theory, without ever using any experimental setup? We can!

1 Historical and educational introduction

Chemistry students must quickly learn to switch between the microscopic and the macroscopic world, which demands from them a high degree of abstraction. In the morning lecture they deal with  and in the afternoon lab course they distil water and determine its boiling point. It is not only that they switch between two levels of different scale, but at the same time they switch between one isolated molecule and a collection of interacting molecules. In addition, in organic chemistry they usually assign in their mind the properties of the isolated molecule to the ensemble of the liquid, and if the discrepancy between the two is too great they invoke the concept of 'solvent effects', which is a nice name for this discrepancy.

In physical chemistry they learn how microscopic or molecular properties can be calculated using quantum mechanics. Thermodynamic laws are taught which relate different macroscopic properties to each other and, finally, some statistical thermodynamics is introduced to show how the microcosmos relates to the macrocosmos, providing the bridge needed to make the switch between the two. Mostly, statistical thermodynamics is limited to the basics—ensembles, partition functions, Boltzmann's law, the calculation of thermodynamic energies and entropy from the partition function—and applications to the ideal gas. The more interesting task, the calculation of properties of real gases or liquids, is usually neglected. This situation could change soon, as several conditions have now been fulfilled which together make this area more amenable to interesting calculations, both in research and in teaching. Let us follow the historical development of the three basic fields necessary for a new approach: quantum chemistry, simulations, and the combination of both with statistical thermodynamics to obtain macroscopic properties.

The birth of quantum chemistry dates back to the late 1920's when the hydrogen bond was interpreted by Heitler and London using valence bond theory, followed a few years later by Hückel's development of his molecular orbital approach. But for the present purpose, *i.e.* quantitative calculations of molecular and intermolecular properties, the real breakthrough came in the 1960's, when semiempirical programs became available and *ab initio* calculations of quantitative accuracy

Hanspeter Huber graduated in 1968 from the Swiss Federal Institute of Technology (ETH) in Zurich, and received his doctoral degree in 1972 for his experimental work in NMR spectroscopy at the University of Basel with Dr C. Pascual and Professor E. Heilbronner. After a post-doc year with Professor J. D. Roberts at Caltech, he changed to quantum chemistry during a subsequent post-doc stay at the Czechoslovak Academy of Science, in the group of Professor R. Zahradník in Prague. Back in Switzerland he returned, after a year of teaching at a grammar school, to the University of Basel, for a 'Habilitation' working on floating orbital geometry optimisation. In 1992 he was appointed Professor of Chemistry. In the last decade he has become interested in the combination of quantum chemistry with simulations to calculate bulk properties of liquids and solvent effects.

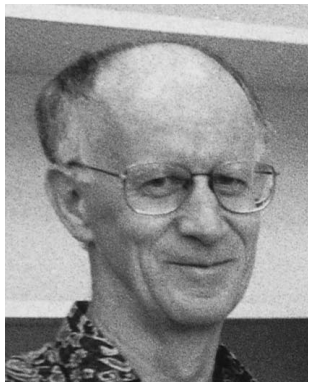

Hanspeter Huber

Barbara Kirchner started her studies of chemistry at the Albert-Ludwigs-Universität in Freiburg, Germany. After completing her Vordiplom she moved to the Johannes Gutenberg-Universität in Mainz, Germany, where she undertook her Diplom thesis in theoretical chemistry, working in the field of density matrix theory. Since 1995 she has been a graduate student of Hanspeter Huber in Basel, Switzerland.

Barbara Kirchner

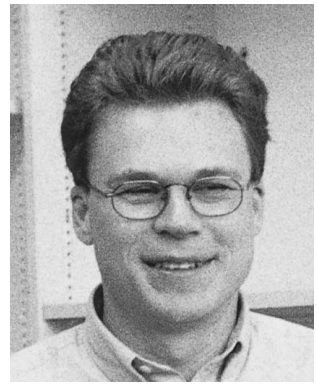

Anthony Dyson

Anthony Dyson received his PhD degree in 1997 from the University of Newcastle, Australia, for work modeling gas–surface interactions. He is currently a post-doctoral research associate at the Institute of Physical Chemistry, University of Basel, Switzerland.

(albeit mainly for diatomic molecules) became possible. This development was based on work started a decade earlier by people such as Roothan, Boys, Pople and many others, but it was facilitated by the introduction and increasing availability of computers. In the 1970's and 1980's large improvements in correlation methods were made. Hand in hand with the ever increasing computer speed, these improved methods to calculate dispersion energy allowed for the accurate calculation of weak intermolecular interactions, which is the key to the understanding of fluids on a microscopic level.

Whereas in quantum chemistry simple calculations were possible even with mechanical and electrical desk calculators, the field of simulations opened up only when electronic programmable computers became available (for a short history and references see ref. 1). The first molecular simulation was carried out in 1953 on the Los Alamos computer, called MANIAC, by Metropolis *et al*. This simulation was of the Monte Carlo type, which does not yield dynamic information. The first molecular dynamics simulations, in which collections of hard spheres were modelled, were performed by Alder and Wainwright four years later. Work on simulations of molecular liquids was published only towards the end of the 1960's. These early publications opened the door to a flood of papers sufficiently voluminous to prompt the creation of a number of specialised journals over the subsequent two or three decades. Nearly all of these papers deal with empirical simulations, in which a microscopic model is calibrated from macroscopic properties (see Box 1) and, thereafter, the microscopic model is applied to calculate other macroscopic properties (see Box 2). Whereas this might be interpreted as a very clever interpolation between two sets of macroscopic data (through a microscopic step), we will deal here with a one-way approach (Box 2), in which the necessary microscopic information is obtained from quantum chemistry without any experimental data, and the resulting model is then used to calculate macroscopic properties. In this way, macroscopic properties are obtained purely from theory, with no prior reference to experimental measurements.

The microscopic model is simply an interaction potential, often called a potential energy surface (PES). The first such potential parametrized purely by *ab initio* calculations and applied in simulations[2] that we are aware of is the MCY water–water potential published in 1976 by Matsuoka, Clementi and Yoshimine.[3]

Box 1. Forth . . . From the macroscopic to the microscopic world

In this box we demonstrate how one proceeds from bulk properties to the microscopic world of a model potential, using argon as a case study. The results can be compared to experimental data from the microscopic argon dimer system.

STEP 1. Argon crystallizes in a face centered cubic (fcc) lattice with a density of 1.79 g cm^{-3} at 1 K and 1.62 g cm^{-3} at 84 K (melting point). If the shortest distance between two atoms is called r_e, then the side length of the fcc unit cell is $\sqrt{2}r_e$ and its volume $2\sqrt{2}r_e^3$. As the unit cell contains four argon atoms with an atomic weight M of 39.95 g mol^{-1}, its density becomes $4M/(N_A 2\sqrt{2}r_e^3)$ with r_e being the only unknown. Hence, we can calculate the distance r_e. Taking the average of the two numbers given above for the density, we obtain r_e = 380 pm. This agrees within 1% with the dimer equilibrium distance of 376 pm obtained experimentally from rovibronic spectra (P. R. Herman, P. E. LaRocque, B. P. Stoicheff, *J. Chem. Phys.*, 1988, 89, 4535).

STEP 2. The boiling point T_s is the temperature at the equilibrium between the gas and the liquid phase, *i.e.* $\Delta_l^g G^\theta = 0$, and, hence,

$$\Delta_l^g H^\theta = T_s \Delta_l^g S^\theta = \Delta_l^g U^\theta + P\Delta_l^g V \approx \Delta_l^g U^\theta + RT_s$$

The last approximation is based on the fact that the liquid volume is negligible in relation to the gas phase volume and the gas is assumed to be ideal. From the above equation we obtain $\Delta_l^g U^\theta = T_s(\Delta_l^g S^\theta - R)$. Let us now call the interaction energy between two argon atoms (*i.e.* the depth of the interaction potential) ε. This is the energy needed to separate two atoms from their equilibrium separation distance, corresponding approximately to the situation in the solid or the liquid, to infinity, corresponding to the gas. The total energy used for the vaporisation is then $\Delta_l^g U^\theta = \frac{1}{2}\varepsilon N_{neighbour}$ (the division by two accounts for the fact that the interaction energy is for a pair of atoms). Combining this with the above result we have $\varepsilon = 2T_s(\Delta_l^g S^\theta - R)/N_{neighbour}$. Assuming 12 neighbours as in the fcc lattice, and assigning with Trouton's rule $\Delta_l^g S^\theta$ = 85 J mol^{-1} K^{-1}, we obtain from the experimental boiling point of 87 K a value for ε of 1112 J mol^{-1} or ε/R = 133.7 K. This is in reasonable agreement with the experimental value for the dimer of 142.7 K (Herman *et al.*, see above).

The results of steps 1 and 2, r_e and ε, can now be used to construct the Lennard–Jones potential shown in the figure below. The equation for such a potential can be written in the two following ways:

$$V(r) = 4\varepsilon\left[\left(\frac{\sigma}{r}\right)^{12} - \left(\frac{\sigma}{r}\right)^{6}\right] \text{ or } V(r) = \varepsilon\left[\left(\frac{r_e}{r}\right)^{12} - \left(\frac{r_e}{r}\right)^{6}\right]$$

where σ is the distance at which the potential is zero. Its value is obtained by division of r_e by the sixth root of two, as can be deduced from the above equations.

To make things even simpler the potential could be approximated by a square well potential, as shown in the figure. The depths of the potentials are identical and σ = 339 pm is now assigned to the distance of closest approach. The right wall of the well is chosen somewhat arbitrarily at a distance where the Lennard–Jones well decays to 1/*e* of its deepest value. This defines the third parameter σ' of the square well potential to be 495 pm.

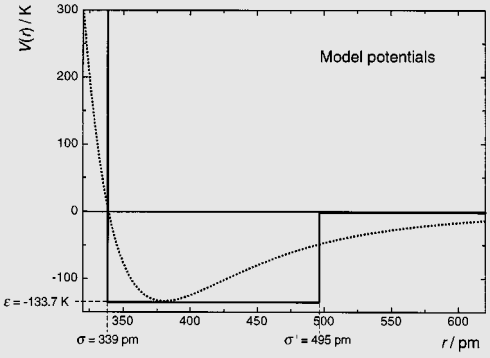

The force constant k can now be calculated from the Lennard–Jones potential as the second derivative of V at the equilibrium distance r_e. This yields $k = 72\varepsilon/r_e^2$, or together with the reduced mass μ of the argon dimer, a wavenumber $\omega = 1/(2\pi c)(k/\mu)^{-1/2}$ = 28 cm^{-1}, which is in good agreement with the experimental value of 30.7 cm^{-1}. The extremely different shape of the square well potential would not lead to reasonable agreement for this property, as one would infer from the figure.

Box 2 . . . and back. From the microscopic to the macroscopic world

In this box we apply the simple square well model potential obtained in the first box to calculate macroscopic properties, specifically the second virial coefficient and the sound velocity.

The second virial coefficient B of a real atomic gas is directly related to the potential by the following equation:

$$B = -2\pi N_A \int_0^\infty \left(e^{-V(r)/RT} - 1\right) r^2 dr$$

With the square well model potential we can easily calculate this integral:

$$\begin{aligned} B &= -2\pi N_A \left[\int_0^\sigma \left(e^{-\infty} - 1\right) r^2 dr + \int_\sigma^{\sigma'} \left(e^{-\varepsilon/RT} - 1\right) r^2 dr \right] \\ &= -2\pi N_A \left[\left[-r^3/3\right]_0^\sigma + \left(e^{-\varepsilon/RT} - 1\right)\left[r^3/3\right]_\sigma^{\sigma'} \right] \\ &= \frac{2}{3}\pi N_A \left[\sigma'^3 - \left(\sigma'^3 - \sigma^3\right) e^{-\varepsilon/RT}\right] \\ &= 153 - 104 e^{133.7/T} \text{cm}^3 \text{ mol}^{-1} \end{aligned}$$

This yields the curve which is plotted and compared with experimental values in the following figure:

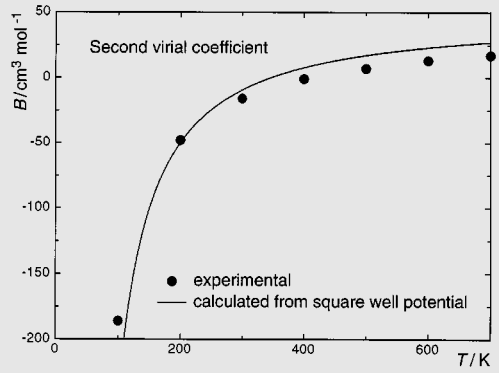

The sound velocity v of a real gas is given by

$$v = V_m \left[-\frac{5}{3M} \left(\frac{\partial P}{\partial V} \right)_T \right]^{\frac{1}{2}}$$

where V_m is the molar volume. Applying the derivative to the virial series we obtain to second order

$$\left(\frac{\partial P}{\partial V} \right)_T = -RT \left(\frac{1}{V^2} + \frac{B}{2V^3} + \cdots \right),$$

and hence

$$v = \left[\frac{5RT}{3M} \left(1 + \frac{B}{2V_m} \right) \right]^{\frac{1}{2}}.$$

With B obtained as described above from the square well potential, the sound velocities shown in the figure below were calculated. The experimental points were obtained from the work of Ewing *et al.* (M. B. Ewing, A. A. Owusu and J. P. M. Trusler, *Physica A*, 1989, 156, 899).

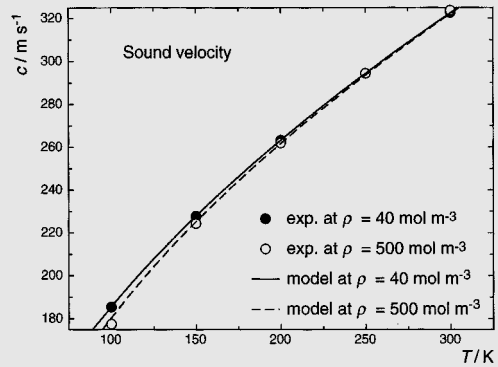

Other properties are obtained similarly. See for example Hanson's determination of the Joule–Thompson coefficient (M. P. Hanson, *J. Chem. Educ.* 1995, 72, 315).

Since then Clementi and coworkers have been working along this line right up to the present time, continuing to produce improved potentials, and studying the influence of different potentials on the calculated properties of water. Their early efforts were made possible only with computer time grants from the then dominating company in the field, IBM. It was less than twenty years ago that this approach also became feasible for groups at universities. An early paper was by Jönsson, Karlström and Romano[4] on nitrogen. However, only a few such papers appeared during the 1980's, and it was only with the recent wide access to supercomputers and high performance workstations that a notable increase of output in this field has been observed.

What was feasible with only the most powerful computers about 20 years ago can now be performed on workstations priced at a few thousand pounds. Within a few years every student will be able to calculate liquid properties of simple systems with fair accuracy, purely from theory, on his or her own desk.

2 What are the tools?

As mentioned in the last paragraph, the necessary hardware consists only of a fast workstation. As software we need a quantum chemistry package and a simulation package, and we will also need to do some straightforward programming work to build our quantum chemically calculated potentials into the simulation code. The latter might be of the Monte Carlo or the molecular dynamics type. We will deal here only with molecular dynamics (MD) simulations, but many of the properties we discuss can also be determined using Monte Carlo simulations.

The standard route by which one proceeds from a microscopic theoretical description to a macroscopic quantity is shown in the movie-like Fig. 1, and consists of the following steps:

a. Selection of a quantum chemical calculation method for the determination of interaction energies;
b. *Ab initio* determination of interaction energies for a series of conformations;
c. Fitting of an analytical PES to the calculated energies;
d. Performance of molecular dynamics simulations using the analytical PES.
e. Analysis of the results, using statistical mechanics, to obtain the macroscopic properties of interest.

The initial task is the construction of the analytical PES (steps a–c from Fig. 1), describing the quantum chemical interactions between the microscopic bodies making up the fluid. The term 'body' is here used for the smallest entity of the liquid, *i.e.* an atom in the rare gas case and a molecule otherwise. The vast majority of PES's currently in use are pair potentials, in which the total energy is approximated as a sum over pair interactions, ignoring the effects of further bodies on each pair interaction.

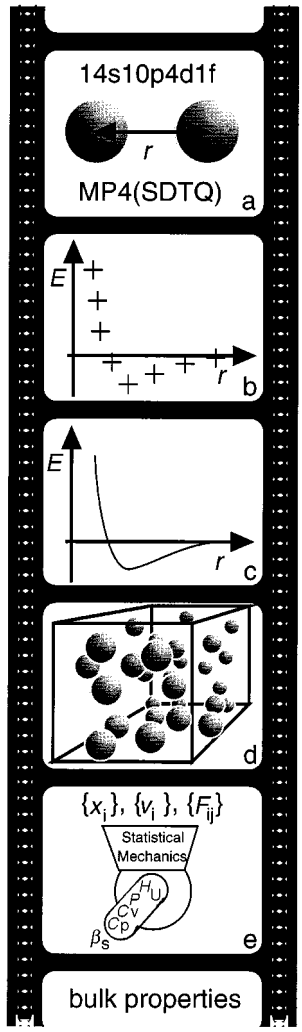

Fig. 1 Going from the microscopic to the macroscopic.

Although we later discuss work in which three-body interactions were also included, we restrict our discussion at this point to the construction of pair potentials.

One must first carefully select an appropriate level at which to perform the quantum chemical calculations of energy (step a). This decision involves the selection of both a method and a basis set. The captions MP4(STDQ) and 14s 10p 4d 1f in Fig. 1a represent typical choices of each for use in calculating the energy of a neon dimer.

For each given relative conformation of two bodies (in the rare gas case just a given distance), the interaction energy is calculated using what is called the 'supermolecular' method, as follows: the dimer energy E_d and the monomer energies E_{m1} and E_{m2} are each calculated *ab initio* using quantum chemical techniques, and the interaction energy is then given by the difference $E_d - (E_{m1} + E_{m2})$ between them. Due to the limited basis sets used to represent the electronic wavefunctions, a so-called basis set superposition error (BSSE) is introduced, which is normally taken care of by the counterpoise correction (for a review see ref. 5). The interaction energies tend to be very small, requiring great precision in the calculations. Some have compared this approach to measuring the weight of an airline pilot by weighing an Airbus with and without the pilot, and taking the difference. This astonishing picture is actually only adequate if we are dealing with relatively strong, intramolecular bonds. If we deal with a typical intermolecular energy, it is more appropriate to compare with the hand baggage of the pilot. For a neon–neon interaction, which is particularly weak, the interaction energy corresponds in this picture rather to a block of Swiss chocolate in the hand of the flight attendant. Reaching chemical accuracy means determining the weights of Airbus with and without chocolate bar with an accuracy of just one square of chocolate! Clearly this places extremely stringent demands on the accuracy of the measurements, which, in the case of quantum chemical calculations, requires the use of extensive basis sets and a high level of theory. Several efforts are underway to develop methods of calculating these interactions without the complications just described. For example, BSSE-free methods include the symmetry adapted perturbation theory (SAPT),[6] the chemical hamiltonian approach (CHA) by Mayer, in some cases supplemented by perturbation theory,[7] and an additional method developed in Raimondi's group.[8,9] Such methods appear promising for future work.

A further complication in the calculation of intermolecular (or interatomic in the case of the rare gases) interaction energies is the fact that usually dispersion energy makes up a high percentage. Only in systems with strong interactions, such as hydrogen-bonded or ionic systems, is a calculation at the self-consistent field (SCF) level reasonably accurate. In all other cases electron correlation has to be included, which means much longer computing times. Density functional theory (DFT) would offer a cost-effective alternative, but the present functionals are not able to yield the dispersion energy even qualitatively correctly (for a first step to improve this situation, see ref. 10).

We now turn out attention to the form of the PES. In the case of rare gases, the pair potential is a one-dimensional curve (see Fig. 1b) and an analytical fit of high accuracy is obtained with 10 to 15 energy points. In contrast, the general intermolecular potential for molecules is a six-dimensional hypersurface, even in the usual approximation where the monomers are kept rigid. Normally, hundreds of points are necessary for the accurate description of such a surface. To choose the number of points and the important conformations, usually rough rules of thumb are applied. (We are, however, aware of two papers whose authors tried to be more systematic in this respect.[11,12])

Having calculated the necessary energy points on an adequate quantum chemical level, an analytical form has then to be found which can be fitted with high accuracy to these points (step c). This is an easy task for a one-dimensional curve, but no trivial problem for a multi-dimensional hypersurface. Once the analytical function has been found and carefully fitted, it is built into the simulation program.

Once the PES has been constructed and coded, simulations can be performed (step d). A molecular dynamics (MD) simulation is usually started from some arbitrary configuration. The evaluation of the energy and the forces on each body for this initial configuration of bodies, and indeed for all of the configurations generated during the simulation, is straightforward and efficient, requiring simply the evaluation of the analytical PES function. Using Newton's 2nd law we then obtain, from the force and mass, the acceleration of each particle, and from this the change in velocity over a small time step. In turn, from the velocity we get the change in location of a particle over the same time step. Working with small time steps in this way is nothing other than a numerical integration of Newton's laws of motion. The time evolution of the system can be followed for as long as desired, so far as computational resources permit.

To obtain thermodynamic properties usually equilibrium simulations are performed. The most often used ensemble in equilibrium simulations is the microcanonical (*NVE*) ensemble, in which the number of bodies (*N*), the volume (*V*), and the energy (*E*) are all constant. An MD simulation of reasonable length is generally thought to sample the ensemble sufficiently that acceptable thermodynamic averages can be obtained. Typically a few hundred to a few thousand particles are used, and *V* is chosen to conform to a selected density. The energy remains constant by virtue of the conservative nature of the potential, but is only indirectly chosen, through the choice of the mean simulation temperature *T*. Non-equilibrium simulations,

in which the configurations generated do not belong to any well defined thermodynamic ensemble, may be usefully performed for investigating phase transitions or transport properties, for example. There are many details to be taken care of in both equilibrium and non-equilibrium simulations which we do not discuss here, such as periodic boundary conditions, different integration algorithms, initial equilibration, and so on. The interested reader is referred to the excellent book of Allen and Tildesley.[1] One thing we would like to emphasise is that all the approximations of the simulation itself, such as finite time step, limited particle number *etc.*, which we might call 'technical errors,' can be relatively easily reduced such that they are negligible, so the only error sources remaining are the approximations listed in Box 3.

Box 3. How sensitive are fluid properties to:

- **the quality of the quantum chemically calculated pair potential?**
- **the neglect of many-body interactions?**
- **the neglect of translational quantum effects?**
- **the neglect of vibrational quantum effects?**
- **the additivity approximation between intra- and intermolecular potentials?**

The first three questions are quite general and will be addressed in this review. The last two are of importance for molecular fluids, but will not be discussed in detail as we do not yet know much about them.

In addition to these error sources, other approximations are made in the simulations which we call 'technical errors', such as the use of a finite time step and restricted numbers of particles, *etc.* Choosing appropriate values for the various technical parameters, these technical errors can always be made negligible compared to the systemic error sources listed above.

After equilibrium in a simulation is reached, it is carried on for typically 10 000 to 100 000 steps and data—such as the location of, velocity of, and forces on each particle—are stored for evaluation (step e). Typical properties one wants to obtain from such an *NVE* simulation at a given density and temperature are, for example, the pressure P, the internal energy U, or the molar heat $C_{V,m}$. The internal energy U in a classical approximation is easy to obtain, as it corresponds directly to the energy E. Usually it has to be transformed to a different zero point of energy and some quantum corrections have to be applied for the vibrations in molecular liquids. The pressure P is given by eqn. (1). It consists of a kinetic or ideal gas part,

$$P = \frac{1}{V}\left(Nk_BT + \frac{1}{3}\sum_{i=1}^{N} r_i F_i \right) \qquad (1)$$

obtained easily from the particle velocities (*via* the temperature), and a potential or non-ideal part calculated from the locations of (r_i) and forces on (F_i) the particles. The third property mentioned above, the molar heat, is given by eqn. (2),

$$C_{V,m} = \frac{3}{2}R\left[1 - \frac{2}{3}\frac{N}{R^2 < T >^2} < \delta E_{kin}^2 >\right]^{-1} \qquad (2)$$

with the usual symbol definitions, and $< \delta E_{\mathrm{kin}}^2 >$ being the variation of the kinetic energy.

The relatively straightforward process described thus far takes on some additional complexity when molecular fluids are the system of interest. As most *ab initio* intermolecular potentials can only be calculated with the monomers kept rigid due to the high dimensionality of the problem, either one has to keep the molecules rigid in the simulations as well, or one has to add an intramolecular potential, hence assuming a further additivity. When flexible molecules are used, one has to be extremely careful that all of the molecular internal degrees of freedom are in equilibrium and, depending on the data evaluation scheme, that the simulations are longer than the energy transfer time between the different degrees of freedom.[13] Further difficulties arise for flexible molecules when calculating properties from fluctuations in energy, such as eqn. (2) for the molar heat. The high frequency intramolecular vibrations tend to introduce strong periodic fluctuations, which introduce large statistical errors. However, alternative ways of data evaluation are often available. For example, the molar heat $C_{V,m}$ can also be calculated as the numerical derivative of the internal energy U with respect to temperature.

To end this section we would like to include a paragraph about the Car–Parrinello method of performing first principles MD simulations. In these simulations, the intermolecular interactions are calculated quantum chemically at each step of the simulation, for the entire system. In this way, many-body effects are inherently included. At present, such calculations are only possible using for the quantum chemical calculations a density functional approach with plane wave basis functions. Although this might change in the future, for the moment DFT calculations are only adequate for strong intermolecular interactions, such as ionic interactions or hydrogen bonded systems. Even then, these simulations are extremely time consuming, and only properties which can be obtained from relatively small ensembles and short runs, such as g-pair distribution functions, have been calculated so far.

3 Applications

3.1 Rare gases

The discussion for the rare gases neon and argon given here is structured around five groups of properties, which each behave differently with respect to the different approximations. The five groups are: the fluid structure represented by the g-pair distribution function, transport properties, the thermodynamic energies and state function, properties derived from those (also in the mathematical sense of derivatives), and the melting curves.

The neon work was based on two different *ab initio* PESs,[14] NE1 and NE2, which are compared in Fig. 2 with a purely empirical pair potential by Slaman and Aziz. Based on many pair properties it was deduced that the step from NE2 to the exact potential is similar to or smaller than the step between NE1 and NE2. This allows us to estimate the improvement which one could expect from a further improvement in the pair potential and, hence, whether such an effort is worthwhile. In the argon work a potential by Woon[15] was employed, which has a very similar quality level as the NE2 neon potential.

Structure. Calculated g-functions for neon at three liquid points where experimental curves are available showed that the overall agreement with experiment is fair, the only discrepancy being the height of the peak corresponding to the first shell. Going from NE1 to NE2 hardly changed the results,[14] indicating that an error source other than the pair potential must be responsible. Simulations including quantum effects in an approximate manner (quantum effective potentials by Wigner and Kirkwood) showed that these accounted completely for the discrepancy.[16] Fig. 3 shows the experimental g-function in comparison with our simulated curve for liquid argon. Similar results were obtained not only for the liquid neon points, but also for argon in the supercritical state at 380 K at different pressures.[17] A three-body potential for neon was also applied, in order to show directly the negligible size of the many-body

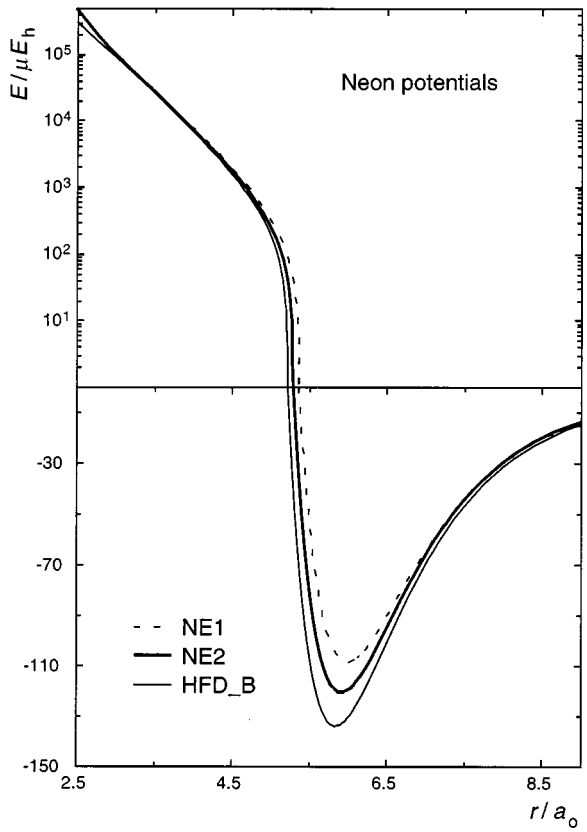

Fig. 2 Comparison of neon pair potentials. NE1 and NE2 are *ab initio* potentials of different quality and the HFD_B potential is a well known empirical pure pair potential by Aziz and Slaman, which is assumed to be virtually exact.

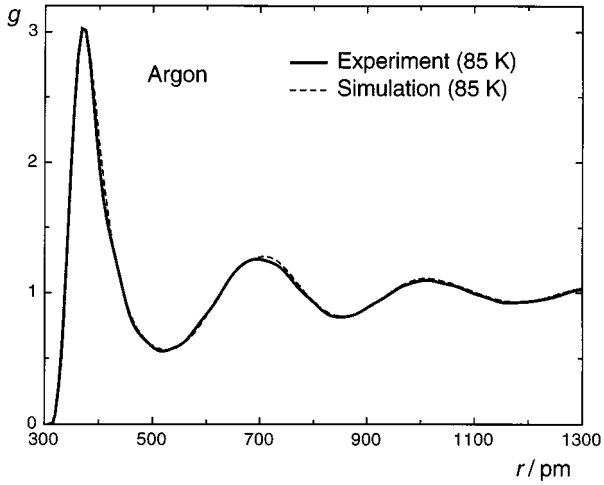

Fig. 3 Comparison between the *g*-pair distribution function from experiment and that obtained by simulation with an *ab initio* quantum chemical potential for liquid argon.

effects.[16,18] The overall conclusions for the structures of fluid neon and argon are: (a) a fairly good pair potential is sufficient; (b) many-body effects are negligible; (c) quantum effects are important at low temperatures.

Transport properties. Even though extremely long simulations were performed for the transport properties,[14] the statistical errors for the thermal conductivity and the viscosity were still large, typically between 5 and 10%. The diffusion coefficient was obtained more accurately, because the trajectory of each particle provides a data point, whereas the other properties require the trajectory of the entire system.

Fig. 4 shows the calculated *versus* the experimental viscosity of neon at 300 K in the supercritical state, for pressures between 100 and 1000 MPa, in increments of 100 MPa (the viscosity increases with the pressure). The error bars are standard deviations. As is easily seen, the calculated and experimental values agree to within two standard deviations. There might be a small trend to disagreement at very high pressures, but it is not statistically significant. Even more in agreement are the values from the two different potentials, showing that an improvement can probably not be expected from an improved pair potential, but that any real deviations at high pressures would be due to many-body effects. A plot of the thermal conductivity shows exactly the same picture.

Table 1 shows values of the transport properties for four liquid points at low temperature, obtained with the two pair potentials without quantum corrections. Again for the viscosity and the thermal conductivity no difference is produced from the different potentials. The diffusion coefficient, on the other hand, seems to increase by roughly 10% with the improved potential. We will give a more sophisticated discussion of this property in the next section. It is somewhat difficult to make a meaningful comparison between the values obtained with the different potentials, and even more so with the experimental values, as the equations of state do not agree well in the liquid at this level of calculation, leading to quite different pressures at a selected NVE point. In spite of this problem, the agreement obtained was reasonably good.

Fig. 5 is an Arrhenius plot of diffusion coefficients determined from experiment, and calculated at different levels of sophistication.[19] The experiments, by Henry and Norberg, were performed at low pressures (about 1 bar). The calculated points are extrapolations to zero pressures from series' of simulations performed at moderate pressures. The values obtained from the NE1 potential are about 50% too large. The improved potential, NE2, lowers this error to about 10%. Including the three-body interaction (TBI) brings the results into perfect agreement with experiment. However, at these low temperatures quantum effects should also be considered. For technical reasons they could not be combined with TBI, and were instead included as a quantum effective pair potential using the method of Wigner and Kirkwood (WK). Nevertheless, it is clear that they worsen the agreement. If we assume additivity between the three-body effects and the quantum effects, which is probably a good approximation, the resulting values would be about 25% too large. The only space for improvement left seems then to be a further refinement of the pair potential and, regarding the large effect going from NE1 to NE2, this might bring the calculated points back into agreement with experiment.

In conclusion, for the viscosity and the thermal conductivity of neon (and similar results were obtained for argon[20]) we can say that within the relatively large statistical error of 5 to 10%: (a) a fairly good pair potential is sufficient; (b) many-body effects are negligible; (c) quantum effects are negligible.

The diffusion coefficient of neon, which was obtained with a very small statistical error, is not known experimentally for the supercritical state and, hence, no comparison is possible. In the liquid state: (a) an excellent pair potential is needed; (b) many-body effects lower the coefficient by about 10%; (c) quantum effects increase the coefficient by about 25%.

Pressure and energies. The energies and, even more so, the pressure were found to be the most sensitive properties to all of the error sources investigated.[14,20] Fig. 6 shows the difference between simulated and experimental pressure at 300 K in the supercritical phase for densities corresponding to experimental pressures of 100, 400, 700 and 1000 MPa. Let us first compare the deviations between the results obtained from the two pair potentials. From such a comparison, it is evident that the growing deviation with increasing pressure does not necessarily imply that many-body interactions play a major role. The improved pair potential NE2 lowers the parabola in such a way

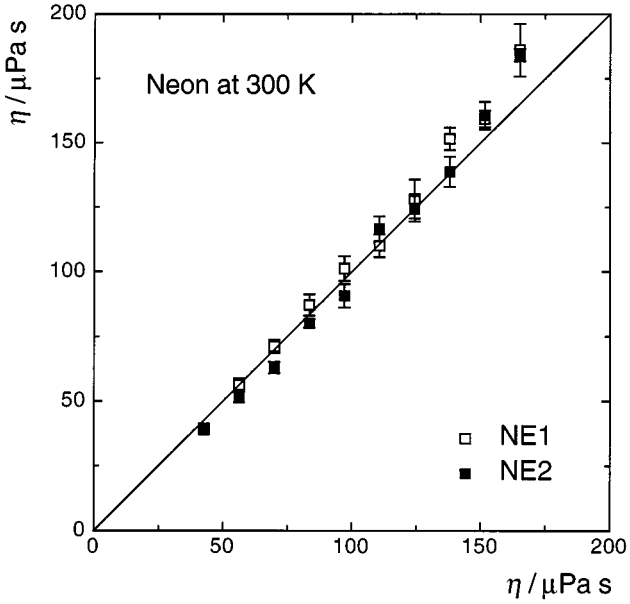

Fig. 4 Simulated *versus* experimental viscosity for supercritical neon at pressures between 100 and 1000 MPa.

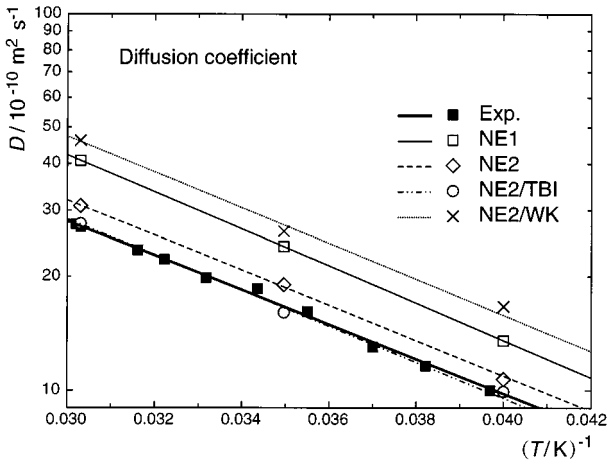

Fig. 5 Arrhenius plot of the diffusion coefficient for liquid neon (see text for a description of the various curves).

that one could even conclude that an exact pair potential would yield exact pressures. Solving the Percus–Yevick equations for a hard sphere model analytically shows a similar dependence, with the main parameter affecting the curvature of the parabola being the size of the spheres.

The inclusion of the TBI, however, leads to a non-parabolic dependence. The overall agreement is excellent—with a deviation of about 1%, chemical accuracy has been reached. A more refined discussion should, however, take into account that an exact pair potential would probably lower the pre-TBI deviation by an estimated two or three percent, hence leading to overly small pressures once TBI is included. At the same time

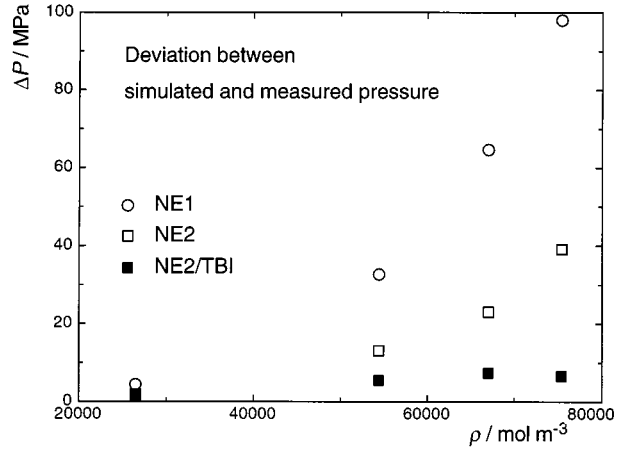

Fig. 6 Deviations between simulated and experimental pressures *versus* density for neon at 300 K (the densities correspond to experimental pressures of 100, 400, 700 and 1000 MPa; technical details of the various simulations are discussed in the text).

though, a second order perturbation calculation gives an estimate of a slightly more than 1% increase due to translational quantum effects, partially balancing this decrease. It may surprise the reader that at 300 K translational quantum effects should play a role. The extremely high pressures lead in fact to a 'cage effect', so that the translation of each atom approximates a vibration within this cage.

Fig. 7 shows another interesting feature of the deviation between the experimental and calculated pressure. The pressure, shown at constant density as a function of temperature in the liquid and supercritical state (T_{crit} = 44.4 K), always manifests the same absolute deviation, regardless of whether the fluid is above or below the critical temperature. The calculated values were obtained with the NE2 potential and corrected for quantum effects by a second order perturbation calculation. The same feature was also observed at higher temperatures for

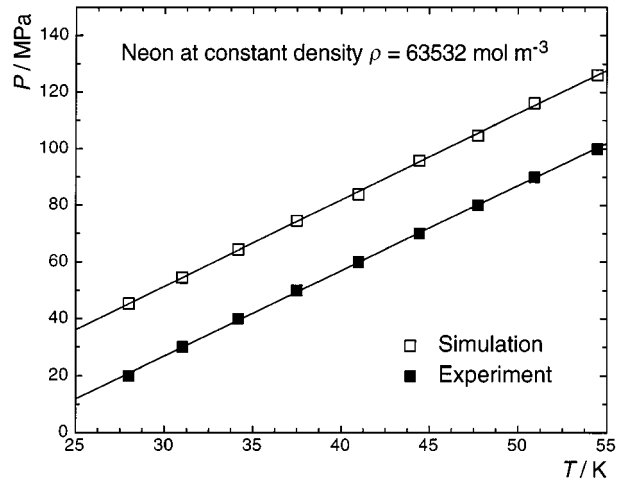

Fig. 7 Deviation in pressure for liquid and supercritical neon *versus* temperature at constant density.

Table 1 Transport properties of liquid neon. The errors are given in parentheses in units of the rightmost digit

		$D/10^{-10}$ m² s⁻¹		λ/Wm⁻¹ K⁻¹			η/μPa s		
T/K	ρ/kg m⁻³	NE1	NE2	NE1	NE2	exp[a]	NE1	NE2	exp[a]
26	1224	12.2 (1)	13.7 (1)	0.134 (4)	0.137 (6)	0.133	135 (4)	121 (3)	150
28	1189	15.6 (1)	17.4 (1)	0.129 (4)	0.119 (2)	0.124	117 (3)	108 (3)	131
36	1043	34.9 (1)	37.3 (1)	0.099 (3)	0.094 (2)	0.092	66 (2)	59 (1)	71
44	942	55.5 (2)	57.9 (1)	0.079 (3)	0.080 (3)	0.077	44 (1)	47 (1)	52

[a] The experimental values can be compared only roughly to the simulated ones as the NE1, NE2 and experimental equations of state are quite different for the liquid. A more detailed comparison is made for the diffusion coefficient in Fig. 5.

argon. This behaviour leads to the situation that in the given example the 33 MPa magnitude of the absolute error at 298 K is comparable to the 28 MPa error at 28 K; however, while the relative error is only 5% at 298 K, it rises to 140% at 28 K (experimental pressure 20 MPa). The situation would be even worse for a liquid at 1 bar!

Table 2 shows thermodynamic energies for neon as a function of pressure. Where experimental values are available, they deviate less than 2% from the calculated ones. The latter, including TBI, can be used as accurate predictions of energies at pressures where no experiments have been performed. Note that even here the inclusion of many-body effects is far less important than the use of a very accurate pair potential. The largest influence due to TBI (at 1000 MPa) for the internal energy is only slightly more than 2%, whereas the improvement of the pair function from NE1 to NE2 (data not given here) yields at the same state point a 5% change.

Table 2 Internal energy and enthalpy for neon at 298 K, in J mol^{-1}

P/MPa	ρ/mol m^{-3}	U_{exp}	U_{sim}	H_{exp}	H_{sim}
100	26 472	3372	3424	7110	7258
400	54 411		3422	10 763	10 875
700	66 998		3688	14 369	14 247
1000	75 737		4025		17 380

In conclusion, from the results for neon, which are supported by work on argon, we find that for the pressure and energies: (a) the pair potential should be extremely accurate; (b) many-body effects are sizeable at high densities only; (c) quantum effects at low temperatures are large.[18]

Derived thermodynamic properties. For neon and argon, experience was accumulated in the calculation of molar heats at constant volume and pressure, compressibilities at constant temperature and entropy, the thermal pressure coefficient, the Joule–Thomson coefficient and the sound velocity c. Experimental values against which to check the accuracy are not available for all properties at all state points. Some properties were obtained with small statistical errors (*e.g.* the sound velocity), while others show sizeable statistical errors even after long simulations (*e.g.* the molar heat at constant pressure). However, the overall picture seems always to be similar, and is illustrated in Fig. 8 for the case of the sound velocity.

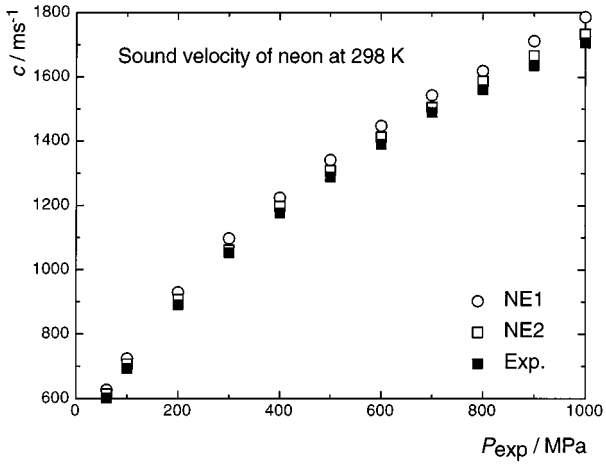

Fig. 8 Experimental and simulated sound velocities *versus* pressure for supercritical neon.

Even with the NE1 potential, the deviation from experiment is only about 5%. The NE2 potential improves the values significantly, decreasing the deviation to less than 2%. Although this is already good, and close to the technical accuracy limit of the simulation, a check for the effect of the TBI was performed with neon. No visible improvement was found. In view of the estimated deviation of NE2 from the exact potential, it seems clear that this does account for the remaining deviation of the derived properties. It may surprise the reader that many-body effects have no influence even at high pressures, in light of their importance for the underlying properties. The reason is probably that the influence of the many-body interactions on the underlying property in question does not change much under slightly changed conditions. For example, the enthalpy obtained from a given pair potential plotted against the temperature at constant pressure gives a curve virtually parallel to the experimental curve. Hence, the slope, *i.e.* the molar heat at constant pressure, is the same for the two curves. In the liquid state of argon between 95 and 145 K, the deviations are, at about 4%, only slightly higher than those of NE2 neon (remember that the quality of the argon potential is close to that of the NE2 potential for neon).

For neon at 28 K the deviation increases to about 25% for the sound velocity, and up to 100% for other derived properties. Given the low temperature, this large deviation indicates the importance of translational quantum effects for properly describing these properties.

Summarising we may conclude for the derived thermodynamic properties that: (a) a good pair potential is needed, but less so than for the pressure; (b) many-body effects are negligible (probably due to cancellations); (c) quantum effects are very important at low temperatures.

Melting curves. Melting curves have been calculated for neon and argon up to about 300 K, with the pair potential only.[21] These investigations were carried out using non-equilibrium molecular dynamics simulations in an *NPH* ensemble (*i.e. N* the number of particles, *P* the pressure and *H* the enthalpy are constant). For neon (see Fig. 9) the highest temperature point

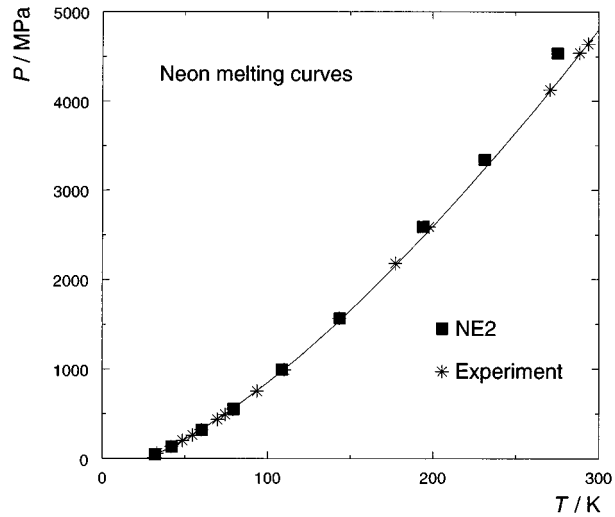

Fig. 9 Experimental and simulated melting curves for neon.

corresponds to a pressure of about 5 GPa, for argon only to about 1 GPa. Whereas the points for argon always deviate by less than 3 K from the experimental ones, which is within the statistical error, the difference between the simulated and the experimental neon curve shows an increasing trend at higher pressures (see Fig. 9), although even there the difference is not more than about two standard deviations. In the simulations one has to be careful to introduce some non-ideality in the starting geometry of the solid, otherwise superheating occurs, and the mechanical instead of the thermodynamical melting point is reached. The results and tests performed showed that: (a) the

pair potential has not to be extremely accurate; (b) many-body effects might be sizeable at pressures higher than 1 GPa; (c) quantum effects are small.

3.2 Carbon dioxide

As pointed out in Box 3, two additional problems arise when modelling molecular systems. First, the additivity between the intermolecular and the intramolecular potential is an approximation, the latter being in the present case only a harmonic approximation itself. Second, the intramolecular vibrational motion is treated classically. At present, we are not able to investigate the quality of these approximations, nor the influence of many-body effects. Fortunately, translational quantum effects can be assumed to be small at the temperatures of interest, *i.e.* not too far away from ambient temperatures. The discussion here focuses on the influence of the quality of the pair potential on the different properties.

Whereas for the rare gases the interaction energy is of purely dispersion type, for carbon dioxide a similar sized contribution due to the electrostatic and inductive interaction of the strong quadrupole moment is expected. This in itself should not be much of a problem for the quantum chemical calculation. The problem is rather that dispersion is still an important contribution, and that for dimers containing six first row atoms it is still not possible to perform calculations of adequate quality to describe dispersion quantitatively. Hence, Domanski *et al.*,[22] having calculated a potential *ab initio*, decided to use it in simulations only after an empirical adjustment. Tsuzuki *et al.* performed *ab initio* calculations on about the best level presently possible, but they used only 40 points to fit the parameters of their ansatz, and for the ansatz itself they selected an empirically approved form, *i.e.* their approach was not directed to produce an unbiased *ab initio* pair potential (for a detailed discussion see ref. 23). Hence, we will report here mainly the results of our group, obtained with two pair potentials,[13,23] and point in only a few cases to the results of Tsuzuki *et al.*[24] Our potentials were calculated on a much finer mesh, with large basis sets contracted to 5s 4p 2d and 8s 6p 4d 1f, respectively, including electron correlation by second order Møller–Plesset perturbation theory (MP2). Whereas the larger basis set is close to saturation with respect to the intermolecular interaction energy, the MP2 level is not adequate to obtain the complete dispersion energy.

Structure. In Fig. 10 simulated and experimental pair distribution functions are compared. The experimental curve was obtained from neutron diffraction measurements, whereas the simulated curve is the neutron-weighted sum of the C–C, C–O and O–O pair distribution functions, obtained from simulations using the better (8s 6p 4d 1f) potential. (Simulations performed using the 5s 4p 2d potential give essentially identical results at these higher densities, but begin to diverge as the density is decreased.) The overall picture shows fair qualitative agreement, as was also found for other phase points.[13] However, there is no quantitative agreement. We assume that carbon dioxide is an extremely difficult case with respect to the structure. The reason is that the dimer has two very different conformations of nearly equal energy. Experiment and calculations now agree that the global minimum is a slipped parallel conformation. However, calculations predict a T-shaped conformation to be a transition state between two slipped parallel conformations, which is probably less than 1 kJ mol^{-1} higher than the minimum. In fact, there are four slipped parallel conformations which are connected by four T-shaped transition states, enabling a planar geared rotation through all eight points, hence leading to a large number of conformations of nearly equal energies with quite different intermolecular structures. For more trivial systems with similar intermolecular forces we might, therefore, expect a reasonable prediction of the pair distribution function from fairly accurate pair potentials, whereas for carbon dioxide the function is a sensitive measure of the details of the potential surface near the minimum and the transition state.

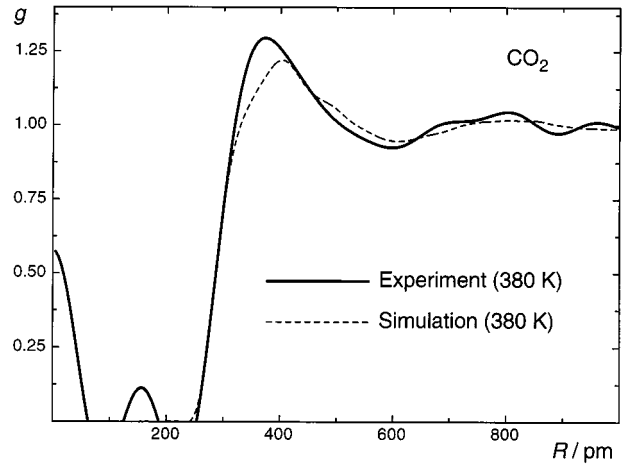

Fig. 10 Comparison of *g*-pair distribution functions for carbon dioxide at a density of 20 455 mol m^{-3}. The simulated curve was obtained with the 8s 6p 4d 1f potential.

Transport properties. The calculation of transport properties, or, more precisely, of the thermal conductivity and the shear viscosity, in equilibrium molecular dynamics simulations is very time demanding. Extremely long runs are required to obtain even modestly small statistical uncertainties. We have calculated a number of transport properties for both liquid and supercritical carbon dioxide,[23] determining each property by two different methods.

The diffusion coefficient was obtained from the Einstein–Smoluchowski relation, and from a time correlation function (Green–Kubo integration). The results are roughly 13% too small. The better potential and the Einstein–Smoluchowski relation seem to yield slightly more accurate values. Tsuzuki *et al.*[24] calculated diffusion coefficients at 323 K for densities up to 19370 mol m^{-3}, which were too small by a similar amount, the largest deviation being 20% for the highest density.

The thermal conductivity was calculated once with an equation valid for rigid molecules, and once by localizing the total energy and momentum of each molecule at its center of mass. The results are roughly the same, but the rigid model shows less statistical error. The values generally agree with experiment to within the statistical errors.

For the shear viscosity, the two evaluations used were identical to those used for the thermal conductivity. Here, in addition, a model where energy and momentum are located on each atom was applied. The results show no conclusive pattern. They are in general slightly larger than the experimental results, but lie roughly within two standard deviations. In conclusion we might state that there is no clear improvement of the calculated values with the better pair potential, and hence the transport properties are not very sensitive to the quality of the pair potential.

Pressure and internal energy. The pressure of a dense fluid is the most sensitive property to any error sources. Fig. 11 shows the experimental pressure, and the pressures calculated from the two different pair potentials at 300 K, *versus* the density. With increasing density the absolute deviation is increasing, but the relative deviation is decreasing. The agreement is much better for the better pair potential, however the relative deviation at the highest density is still 34%. In contrast to the rare gases where the accuracy of the results is relatively high, we are now only

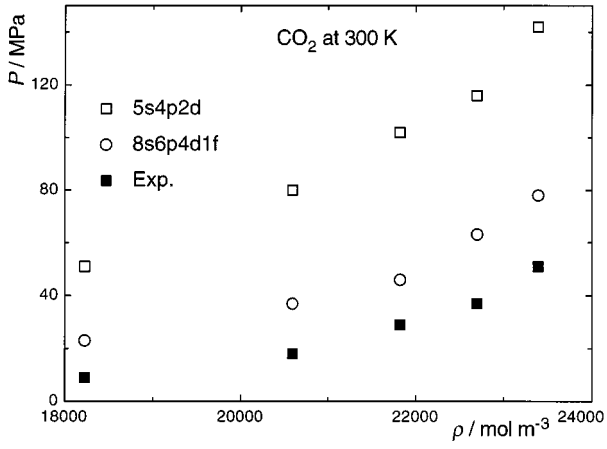

Fig. 11 Experimental and simulated pressures *versus* density for fluid carbon dioxide.

just reaching a point where quantitative calculations for carbon dioxide are becoming possible. At this point we should be careful when drawing any conclusions about the error due to the neglect of many-body interactions. Many authors show an inclination to attribute the deviation of their simulation results from experiment to 'many-body interactions.' However, even the second virial coefficient, which is a pure pair property, shows a strong disagreement between calculation and experiment. For a test calculation the better potential was scaled in the energy axis to fit the experimental virial coefficient, and was then used in a simulation in the liquid state. The pressure was then no longer too large, but decreased to the extent that it even became slightly negative. This demonstrates that an improvement in the pair potential could still strongly change the calculated pressure.

A further indication of the sensitivity of the pressure to the nature of the pair potential is given by the following comparison. Tsuzuki *et al.*[24] have calculated pressures at densities up to 20 000 mol m^{-3} between temperatures of 320 and 400 K. At the highest density and 320 K they obtain a pressure which is 12% too small, whereas at a similar state point the better of our potentials yields a pressure which is 50% too large. Bearing in mind that the potential used by Tsuzuki *et al.* was fitted to accurate MP2-level quantum chemical calculations, as was our potential, the explanation for this astounding difference must lie in the use of an empirically selected ansatz by Tsuzuki *et al.*, along with the extra flexibility in their fit due to the low number of points used.

The internal energy corresponds in a simulation of the microcanonical ensemble to the constant energy E. However, in a simulation with flexible molecules a correction for the vibrations has to be applied as the simulation treats them completely classically. In the work discussed here, this has been done in the most simple way, by subtraction of the classical contribution RT, and addition of the quantum chemical contribution for the harmonic oscillator of the frequency used in the intramolecular potential for each vibrational eigenstate. Whereas for the worse potential the resulting energies are typically 2.5 kJ mol^{-1} (~10%) too large in the investigated range, the deviation from experiment decreases to about 1.1 kJ mol^{-1} (~5%) for the better potential. We hence expect to obtain values close to experiment with an exact pair potential.

Derived thermodynamic properties. The thermal pressure coefficient γ_V and the molar heat $C_{V,m}$ at constant volume were calculated[13] as numerical derivatives of the pressure and internal energy at different state points. The thermal pressure coefficient cannot be compared to experimental values as no such data are available. The experimental molar heats are fairly constant, lying betweeen 39.2 and 42.9 J mol^{-1} K^{-1} over the ranges investigated (from 280 to 440 K at a density of 18 225 mol m^{-3}, and densities from 18 225 to 25 665 mol m^{-3} at 300 K). The calculated values are typically 5 to 10% smaller, which is within the uncertainty limits of the relatively crude evaluation method. No significant difference was observed between the two different potentials, although the values obtained with the better potential seem to be slightly closer to experiment.

3.3 Water

Whereas the rare gases cause some problems due to their extremely weak interactions, we should be aware that they form very simple liquids. Therefore, it might not be so surprising that we obtain quite quantitatively accurate results once the quantum chemical calculation of the interaction energy has reached a reasonable level. Additional problems arise for the molecular liquid carbon dioxide with its internal degrees of freedom, where the vibrations no longer follow the classical laws of motion and the intermolecular potential cannot yet be calculated on the necessary level. However, water is an even more complicated liquid with its hydrogen bonds and, although it has been the subject of most of the *ab initio* investigations carried out in the last two decades, we cannot yet expect even the accuracy that has been reached for carbon dioxide. Due to its high polarity, larger many-body interactions are expected. The hydrogen bonds lead to hindered rotations, hence being the source of sizeable quantum effects even at room temperature. Quantum effects might also play a role in a tunneling and/or zero point vibrational movement of the hydrogen in the hydrogen bond.

For water there have not been as many properties calculated and compared with experiments over wide ranges of phase points as for the other systems we have already discussed. Most work has dealt with only the structure, as it is difficult enough to find agreement between experiment and calculations even for this relatively insensitive property. For water the experimental g function can be resolved in site–site pair distribution functions g_{HH}, g_{OH} and g_{OO}. However, different experiments have yielded quite different functions, and even now the most recent work[25,26] can only be considered semi-quantitative, particularly when it comes to the peak intensities. This important point must be kept in mind throughout the following discussion.

Below we will compare experimental with simulated data from recent work on water. This includes the simulations of Famulari *et al.*[9] which were done with a newly reparameterised version of the NCC-vib potential, originally developed by Nieser, Coringui and Clementi. The reparameterisation was carried out by fitting to *ab initio* BSSE-free calculations for 225 dimer and 28 trimer configurations. We also discuss the work of Liu *et al.*,[27] carried out with a new potential based on relatively few *ab initio* points (94 dimers and 57 trimers), and the work of Corongiu and Clementi[28] in which the NCC-vib potential was used. In both of these studies, partial counterpoise corrections were performed to reduce the BSSE. (This publication of Corongiu and Clementi is not as recent as the others we refer to, having appeared in 1992, but it is based on long experience with *ab initio* water work in that group.) A few results of Car–Parrinello simulations[29,30] obtained with different functionals are also available for comparison. (The work reported in ref. 30 is based on that of ref. 29, and was performed in the same group). The structure used for the comparison below was obtained with a functional due to Becke, Lee, Yang, and Parr (BLYP). These calculations were BSSE-free by virtue of the plane wave basis employed.

Millot *et al.*[31] recently developed two new parametrized polarizable pair potentials based on *ab initio* calculations, which they tested together with 12 other polarizable models from the literature in reproducing pair properties. They report quite promising results, but the potentials have not yet been applied to the condensed phase, preventing any detailed comparison in our

discussion here. For the second virial coefficient they obtain good agreement with experiment between 373 and 973 K when first-order quantum corrections are included. The quantum corrections are substantial, amounting to 10–15% of the classical value at 373 K, 20–25% at 323 K, and 30–35% at 273 K. The SAPT-based potential of Mas *et al.*[6] also gives very good agreement with experiment for the second virial coefficient, with quantum corrections of up to 20%. These results suggest that also in typical liquid simulations quantum effects are substantial, and one has to go beyond classical simulations to obtain quantitative results. This has not been done in the simulations we are about to compare (for a critical discussion see also ref. 32). First steps, although with empirical potentials only, to include quantum effects on a level managable with todays computers were published in the last few years by several groups (see references in ref. 33). Strong quantum effects are observed at ambient temperatures, *e.g.* the pair distribution functions show less pronounced shells, with the peaks flattened by 10 to 20%, as is seen for the rare gases at low temperature (see discussion in Section 3.1). We will include quantum effects in our qualitative discussion of the water structure below, but we are not able to discuss the influence of the other error sources in detail with only the data currently available.

Structure. Fig. 12 shows a comparison between the experimental and calculated pair correlation functions g_{OO}, g_{OH} and g_{HH} at ambient conditions. All potentials correspond to flexible and polarizible water molecules obtained from quantum chemical calculations. The two experimental pair distributions discussed here are the last published curves from Soper,[25] as well as slightly improved curves obtained by reanalysing the same measurements using a refined procedure.[34]

The experimentalists stress that the intensities of the peaks they report are not very accurate, and hence the simulations should not be critically judged by the degree of their agreement with the measured intensities. Soper gives a typical standard error of about 15% for the first peak of each curve, and about half that size for the second peak, with the exception of the second peak of the g_{OO} function, where the error is still about 10%. As is well known, one has to expect that the error of an individual curve is about twice the standard error, and a comparison of the 1997 values of Soper shows indeed a deviation from the new values (obtained from the same experiment) of around that size.

The simulated curves show quite different intensities from one another as well as sizeable deviations from the experimental intensities. However, due to the large uncertainties in the experiment, it is not possible on the basis of these differences alone to discriminate between the qualities of the different potentials. A further cause for uncertainty in a comparison is the absence of quantum effects in all simulations. From empirical simulations we know that the first peaks decrease by about 10 to 20% when quantum effects are included, whereas the prominent second peak in the g_{OH} function is not much affected.

In contrast to the intensities, the radial positioning of the peaks in the experimental curves is considered to be quite accurate. In the region of the first peak, there is a good agreement in the radial behaviour between all curves in Fig. 12. At longer distances, the curves of Famulari *et al.* deviate noticeably from the others. The cause of this deviation is, however, clear. This particular work of Famulari *et al.* is the first application of their new BSSE-free approach, *i.e.* not requiring counterpoise correction, to water. The authors attribute the poor long range behaviour to the absence of sufficient diffuse basis functions in the *ab initio* calculations. Preliminary investigations have shown that extension of the basis set with extra diffuse functions improves the treatment of the long range interactions.[35]

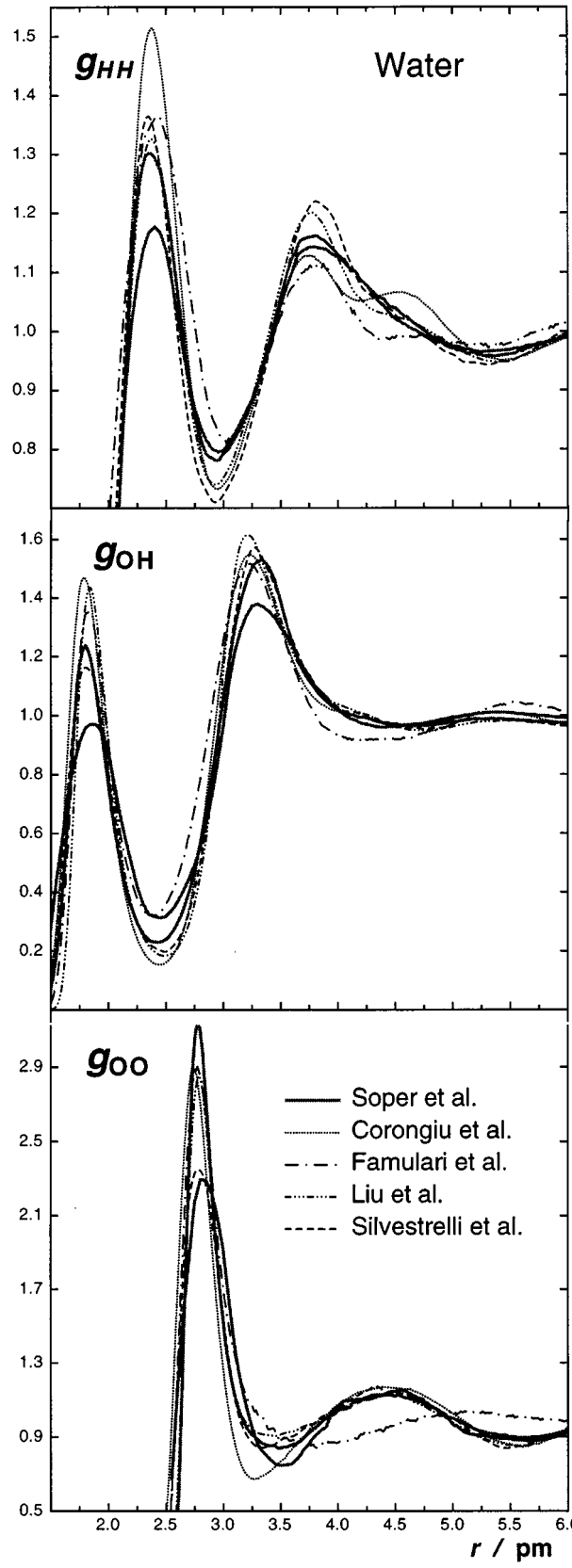

Fig. 12 The g_{OO}, g_{OH} and g_{HH} radial pair distribution functions of water at ambient conditions. The results from four recent simulations are compared with experiment. In each case, two experimental curves are shown. The one with the lower first shell peak intensity is from ref. 25. The other was extracted from the same experimental measurements, but using a refined analysis technique.[34]

Not withstanding this failure of the current Famulari *et al.* potential to reproduce the long range structure, we may say in conclusion that all of the simulations discussed give results in reasonable agreement with the experiment, when the un-

certainties of the quantum effects and the relatively large uncertainties in the experimental intensities are taken into account. On the theoretical side, most future effort should be put into the inclusion of quantum effects, which can probably be successfully done by the application of a perturbation approach such as that used in ref. 16. On the experimental side, a decrease in the standard deviations of the peak intensities is needed, to enable a meaningful comparison with the independently-obtained theoretical results.

Measurements and calculations of the structure at other phase points have also been made, but it would not add greatly to our discussion to go into more details here. The interested reader is referred, for example, to refs. 9 and 26, and references therein.

Transport properties. Liu *et al.* report a diffusion constant at ambient conditions of $1.9 \pm 0.15 \times 10^{-9}$ m^2 s^{-1} and Corongiu[36] one of 2.4×10^{-9} m^2 s^{-1}, compared to an experimental value of 2.30×10^{-9} m^2 s^{-1}. Sprik *et al.*[29] find values of 2.3 (B), 0.035 (BP) and 0.13 (BLYP) $\times 10^{-9}$ m^2 s^{-1} for three different functionals.

Pressure and internal energy. Famulari *et al.* obtain a pressure of 72.4 ± 15.6 MPa at ambient conditions. Although this is a factor 724 too large, it is a great improvement in comparison with previous results obtained with other potentials. The absolute error of 72.3 MPa might be compared to an absolute error of about 25 MPa for carbon dioxide at 300 K and a similar gram-density. Liu *et al.* report a pressure of −60 MPa for water under the same conditions, while the NCC-vib potential yielded −216 ± 36 MPa.

Internal energies are compared for two state points.[9] Both at ambient conditions, where Famulari *et al.*'s calculated value of -40.56 ± 0.22 kJ mol^{-1} corresponds to an experimental value of −41.5 kJ mol^{-1}, and at 573 K and a density of 0.71796 g cm^{-3} (-22.43 ± 0.09 kJ mol^{-1} calculated *vs.* −22.2 kJ mol^{-1} experimental) the agreement is excellent. The simulation was performed using the MOTECC suite of programs developed by Clementi's group, and does not include any quantum correction. 23% Of the potential energy was found to stem from the many-body polarization term, possibly providing an indication of the importance of this term. Liu *et al.* report an internal energy of −42.3 kJ mol^{-1} at ambient conditions. Corongiu obtains a value of −41.4 kJ mol^{-1}, after making an inter- and intramolecular zeroth-order quantum correction.

Derived thermodynamic properties. Famulari *et al.* give a calculated molar heat at constant volume of $C_{V,m}$ = 93 J mol^{-1} K^{-1} at ambient conditions, calculated in the usual way from temperature fluctuations, which must be compared with an experimental value of 75 J mol^{-1} K^{-1}. The large deviation here contrasts with the relatively good agreement for the internal energy. This deviation could be reduced by the inclusion of quantum corrections, which are expected to make non-negligible contributions.[35]

4 Outlook

Yes, molar heat capacities and viscosities of liquids can be calculated purely from theory! In most cases, though, the quality of the results is not yet above all doubt. For the rare gases neon and argon a predictive level has been reached for many properties. For them and the heavier rare gases, as well as for rare gas mixtures, we will probably be able within a few years to calculate any property as accurately as measurements can be performed. For molecular liquids without hydrogen bonds and strong dipole moments, this goal should be reached within the next two decades, for moderately sized molecules and mixtures of them. Thereafter the same quality will slowly but surely be approached for larger systems. For molecules with hydrogen bonds the situation might be more complicated, due to quantum effects in librational motions and the tunneling of the bridge-hydrogen. For such systems, classical simulations might not be adequate to predict other properties than those discussed in this review, as suggested by Brodsky[32] in his somewhat pessimistic letter entitled: 'Is there predictive value in water computer simulations?' In the meantime, the methods that have been discussed in this Review will continue to provide a useful bridge between microscopic theory and the observable world, for the large variety of systems to which they are well suited.

5 Acknowledgements

We would like to thank the authors of refs. 9, 27, 28, 30 and 34 for supplying to us the *g*-pair distribution functions as shown in Fig. 12 in electronic form. In addition, we thank Professor A. Soper for some helpful discussions. This work is part of the project 2000–045269.95 of the Schweizerischer Nationalfonds zur Förderung der Wissenschaften.

6 References

1 M. P. Allen and D. J. Tildesley, *Computer Simulations of Liquids*, Clarendon Press, Oxford, 1987.
2 G. C. Lie, E. Clementi and M. Yoshimine, *J. Chem. Phys.*, 1976, **64**, 2314.
3 O. Matsuoka, E. Clementi and M. Yoshimine, *J. Chem. Phys.*, 1976, **64**, 1351.
4 B. Jönsson, G. Karlström and S. Romano, *J. Chem. Phys.*, 1981, **74**, 2897.
5 F. B. van Duijneveldt, J. G. C. M. van Duijenveldt-van de Rijdt and J. H. van Lenthe, *Chem. Rev.*, 1994, **94**, 1873.
6 E. M. Mas, K. Szalewicz, R. Bukowski and B. Jeziorski, *J. Chem. Phys.*, 1997, **107**, 4207.
7 I. Mayer, *Int. J. Quant. Chem.*, 1998, **70**, 41.
8 A. Famulari, M. Raimondi, M. Sironi and E. Gianinetti, *Chem. Phys.*, 1998, **232**, 289.
9 A. Famulari, R. Specchio, M. Sironi and M. Raimondi, *J. Chem. Phys.*, 1998, **108**, 3296.
10 C. Adamo and V. Barone, *J. Chem. Phys.*, 1998, **108**, 664.
11 J. E. Carpenter, W. T. Yets III, I. L. Carpenter and W. J. Hehre, *J. Phys. Chem.*, 1990, **94**, 443.
12 S. Swaminathan, R. J. Whitehead, E. Guth and D. L. Beveridge, *J. Am. Chem. Soc.*, 1977, **99**, 7817.
13 G. Steinebrunner, A. J. Dyson, B. Kirchner and H. Huber, *J. Chem. Phys.*, 1998, **109**, 3153, and references therein.
14 R. Eggenberger, H. Huber and M. Welker, *Chem. Phys.*, 1994, **187**, 317.
15 D. E. Woon, *Chem. Phys. Lett.*, 1993, **204**, 29.
16 E. Ermakova, J. Solca, H. Huber and D. Marx, *Chem. Phys. Lett.*, 1995, **246**, 204.
17 T. Pfleiderer, I. Waldner, H. Bertagnolli, K. Tölheide, B. Kirchner and H. Huber, unpublished work.
18 B. Kirchner, E. Ermakova, J. Solca and H. Huber, *Chem. Eur. J.*, 1998, **4**, 379.
19 B. Kirchner, E. Ermakova, G. Steinebrunner, A. Dyson and H. Huber, *Mol. Phys.*, 1998, **94**, 257.
20 E. Ermakova, J. Solca, H. Huber and M. Welker, *J. Chem. Phys.*, 1995, **102**, 4942.
21 J. Solca, A. J. Dyson, G. Steinebrunner, B. Kirchner and H. Huber, *J. Chem. Phys.*, 1998, **108**, 4107, and references therein.
22 K. B. Domański, O. Kitao and K. Nakanishi, *Mol. Sim.*, 1994, **12**, 343.
23 G. Steinebrunner, A. J. Dyson, B. Kirchner and H. Huber, *Collect. Czech. Chem. Commun.*, 1998, **63**, 1177.
24 S. Tsuzuki, T. Uchimaru, M. Mikami, K. Tanabe, T. Sako and S. Kuwajima, *Chem. Phys. Lett.*, 1996, **255**, 347.
25 A. K. Soper, F. Bruni and M. A. Ricci, *J. Chem. Phys.*, 1997, **106**, 247.

26 T. Tassaing, M.-C. Bellissent-Funel, B. Guillot and Y. Guissani, *Europhys. Lett.*, 1998, **42**, 265.
27 Y.-P. Liu, K. Kim, B. J. Berne, R. A. Friesner and S. W. Rick, *J. Chem. Phys.*, 1998, **108**, 4739.
28 G. Corongiu and E. Clementi, *J. Chem. Phys.*, 1992, **97**, 2030, and erratum *J. Chem. Phys.*, 1992, **97**, 8818.
29 M. Sprik, J. Hutter and M. Parrinello, *J. Chem. Phys.*, 1996, **105**, 1142.
30 P. L. Silvestrelli and M. Parrinello, unpublished work.
31 C. Millot, J.-C. Soetens, M. T. C. Martins Costa, M. P. Hodges and A. J. Stone, *J. Phys. Chem. A*, 1998, **102**, 754.
32 A. Brodsky, *Chem. Phys. Lett.*, 1996, **261**, 563.
33 B. Guillot and Y. Guissani, *J. Chem. Phys.*, 1998, **108**, 10162.
34 A. K. Soper, personal communication.
35 M. Raimondi and A. Famulari, personal communication.
36 G. Corongiu, *Int. J. Quant. Chem.*, 1992, **42**, 1209.

Review 8/03457E